

# Two-dimensional electron systems beyond the diffusive regime

P. Markoš

*Department of Physics FEI, Slovak University of Technology, 812 19 Bratislava, Slovakia*

Transport properties of disordered electron system can be characterized by the conductance, Lyapunov exponent, or level spacing. Two additional parameters,  $K_{11}$  and  $\gamma$  were introduced recently which measure the non-homogeneity of the spatial distribution of the electron inside the sample. For the orthogonal, unitary and symplectic two dimensional disordered models, we investigate numerically the system size dependence of these parameters in the diffusive and localized regime. Obtained size and disorder dependence of  $K_{11}$  and  $\gamma$  is in agreement with single parameter transport theory. In the localized regime,  $\gamma \rightarrow 0$  independently on the physical symmetry of the model. In the diffusive regime,  $\gamma$  equals to the symmetry parameter  $\beta$ . For the symplectic model we analyze the size dependence of  $\gamma$  in the critical region of the metal-insulator transition and found the non-universal critical value  $\gamma_c$ .

PACS numbers: 73.23.-b, 71.30.+h, 72.10.-d

## I. INTRODUCTION

Transport of electrons through disordered structures offers a broad variety of interesting universal phenomena.<sup>1,2</sup> With increase of the strength of the disorder the character of the transport changes from the ballistic to diffusive up to the insulating, where all electrons are localized.<sup>3</sup>

In the limit of weak disorder (diffusive regime) the transport can be studied analytically using, for instance, the Dorokhov Mello Pereyra Kumar (DMPK) equation<sup>4</sup> the Green's function analysis<sup>5</sup> or random matrix theory.<sup>6,7</sup> The existence of the metal-insulator transition in two and three dimensional models<sup>8,9</sup> is a strong motivation to construct an analytical theory of the transport beyond the diffusive regime<sup>10,11</sup>. Also, numerical data for the localized regime<sup>12-16</sup> show that, contrary to theoretical expectation, the distribution of the logarithm of the conductance is never Gaussian for disordered systems in higher dimension. Therefore, a general transport theory must explain how the dimension of the system and physical symmetry of the model<sup>9</sup> influence the ability of electron to move through the sample.

The most elaborated analytical description of the transport in strongly disordered structures is based on the generalized DMPK equation (GDMPKE).<sup>17</sup> The theory takes into account that the spatial distribution of electrons in the regime of localization is not homogeneous. The last was confirmed by numerical simulations in Ref.<sup>14,18</sup> In GDMPK, the non-homogeneity of electron distribution is measured by a large number of parameters  $K_{ab}$  (defined later); however, only two of them,  $K_{11}$  and  $\gamma = 2K_{12}/K_{11}$  are decisive for the transport.<sup>19</sup>

The GDMPKE is not exactly solvable, but approximate analytical solution for 3D disordered systems<sup>19-21</sup> agrees very well with numerical data. Numerical solution of GDMPKE<sup>22</sup> confirmed that it correctly describes disordered orthogonal systems and that parameters  $K_{ab}$  depend on the dimension of the system.

Detailed numerical analysis of parameters  $K_{11}$  and  $\gamma$  in three dimensional model was performed in<sup>20</sup>. The aim

of this paper is to investigate how these parameters depend on the physical symmetry in two dimensional (2D) models. We present numerical data for the parameters  $K_{11}$  and  $\gamma$  for the orthogonal model (O), unitary (U) and two symplectic (S)<sup>23,24</sup> models in diffusive and insulating regime. For the S models, we also study the behavior of both parameters in the critical regime of the metal-insulator transition.

## II. GENERALIZED DMPK EQUATION

Consider a disordered system of the length  $L_z$  connected to two semi-infinite ideal leads with  $N$  open channels. Transmission parameters are given by the transfer matrix, which can be written in general form as<sup>4</sup>

$$T = \begin{pmatrix} u & 0 \\ 0 & u' \end{pmatrix} \begin{pmatrix} \sqrt{1+\lambda} & \sqrt{\lambda} \\ \sqrt{\lambda} & \sqrt{1+\lambda} \end{pmatrix} \begin{pmatrix} v & 0 \\ 0 & v' \end{pmatrix}. \quad (1)$$

In Eq. (1),  $u, v$  are  $N \times N$  matrices, and  $\lambda$  is a diagonal matrix, with positive elements  $\lambda_a, a = 1, 2, \dots, N$ . In systems with time reversal symmetry, matrices  $u'$  and  $v'$  can be represented in terms of  $u$  and  $v$ .<sup>25</sup> For the orthogonal system,  $u' = u^*$  and  $v' = v^*$ . For the symplectic symmetry, the scattering depends on the spin of the electron; the elements of matrices  $u$  and  $v$  are  $2 \times 2$  matrices which fulfill the symmetry relations<sup>6,25</sup>

$$u' = k u^* k^T, \quad v' = k v^* k^T, \quad k = \begin{pmatrix} 0 & -1 \\ 1 & 0 \end{pmatrix}. \quad (2)$$

Statistical variables  $u, v$  and  $\lambda$  contain entire information about the transport. In the weak disorder limit,<sup>4</sup> the conductance  $g$  (in units of  $2e^2/h$ ) is completely determined by eigenvalues  $\lambda_a$ .<sup>6,26</sup>

$$g = \sum_{a=1}^N \frac{1}{1 + \lambda_a} = \sum_{a=1}^N \frac{1}{\cosh^2 x_a/2} \quad (3)$$

In the last equation, we used the parametrization  $\lambda_a = (\cosh x_a - 1)/2$ .

The probability distribution of  $\lambda$ s can be found as a solution of the DMPK equation.<sup>4</sup> The generalization of the DMPK for the orthogonal symmetry class, was done by Muttalib and Klauder<sup>17</sup> who introduced new parameters,  $K_{ab}$  which characterize the spatial distribution of the electron in the disordered sample. The generalized DMPK equation reads<sup>17</sup>

$$\frac{\partial p_{Lz}(\lambda)}{\partial(Lz/\ell)} = \frac{1}{J} \sum_a^N \frac{\partial}{\partial \lambda_a} \left[ \lambda_a (1 + \lambda_a) K_{aa} J \frac{\partial p}{\partial \lambda_a} \right], \quad (4)$$

where  $\ell$  is the mean free path, and

$$J \equiv \prod_{a < b}^N |\lambda_a - \lambda_b|^{\gamma_{ab}}, \quad \gamma_{ab} \equiv \frac{2K_{ab}}{K_{aa}}. \quad (5)$$

This equation can be simplified when all  $K_{aa}$  are approximated by  $K_{11}$  and  $\gamma_{ab} \approx \gamma$  for all  $a, b$  ( $a \neq b$ ). This approximation was confirmed by numerical work<sup>20,22</sup>.

Although the conductance is still given by Eq. (3), it becomes implicitly a function of the spatial distribution of the electron.

### III. MODELS

In numerical work, disordered sample is represented by two dimensional (2D) square disordered lattice of the size  $L \times L$ . The orthogonal 2D model with on-site disorder is defined by the Hamiltonian

$$\begin{aligned} \mathcal{H} = & W \sum_{xz} \epsilon_{xz} c_{xz}^\dagger c_{xz} \\ & + V_\perp \sum_{xz} c_{x+a,z}^\dagger c_{xz} + c_{xz}^\dagger c_{x+a,z} \\ & + V_\parallel \sum_{xz} c_{x,z+a}^\dagger c_{xz} + c_{xz}^\dagger c_{x,z+a} \end{aligned} \quad (6)$$

Here,  $a$  is the lattice spacing,  $\epsilon_{xz}$  are random energies from the box distribution,  $|\epsilon_{xz}| < 1/2$ ,  $W$  measures the strength of the disorder and  $V_\parallel \equiv 1$  defines the energy scale. To avoid closed channels in leads, we use  $V_\perp/V_\parallel = t < 1$ .<sup>27</sup> In what follows we consider  $t = 0.9$ , the energy of the electron  $E = 0.01$ . With  $a \equiv 1$ , we identify the number of channels

$$N \equiv L. \quad (7)$$

It is generally accepted<sup>2,8</sup> that only localized regime exists in the model when the size of the system  $L \rightarrow \infty$  (the critical disorder  $W_c = 0$ ). Nevertheless, diffusive transport is observable for sufficiently weak disorder and small sample size.<sup>13</sup>

The second model of interest is the symplectic model with spin dependent hopping. Here, the hopping of electron from one site to the neighboring one can be accompanied by the change of the sign of the spin and  $V_\parallel, V_\perp$  become  $2 \times 2$  matrices. In numerical simulations, we study the Ando model with hopping hopping terms

$$V_\perp = t \begin{pmatrix} V_1 & -V_2 \\ V_2 & V_1 \end{pmatrix}, \quad V_\parallel = \begin{pmatrix} V_1 & -iV_2 \\ -iV_2 & V_1 \end{pmatrix}. \quad (8)$$

The spin-orbit coupling is characterized by the parameter  $S = V_1$  and  $V_1^2 + V_2^2 = 1$ . In this paper,  $S = 0.5$ . We also study the Evangelou-Ziman (EZ) model<sup>23</sup> which uses the random hopping matrices  $V$ : with help of three independent random variables,  $t^x, t^y, t^z$ , distributed uniformly in interval  $(-\mu/2, \mu/2)$

$$V_\perp = V_{xz, x+az} = t \begin{pmatrix} 1 + it^z & -t^y + it^x \\ t^y - it^x & 1 - it^z \end{pmatrix}, \quad (9)$$

and

$$V_\parallel = V_{xzxz+a} = \begin{pmatrix} 1 + it^z & -t^y + it^x \\ t^y - it^x & 1 - it^z \end{pmatrix}, \quad (10)$$

and consider  $\mu = 1$ .

Both Ando and EZ model exhibit the metal-insulator transition when the disorder  $W$  reaches the critical value  $W_c$ .<sup>23,24</sup> Owing to the anisotropy of our models, the critical disorder differs from that obtained in previous works.<sup>23,28</sup> We found  $W_c \approx 5.525$  for the Ando model and  $W_c = 6.375$  for the EZ model.

The 2D model with external magnetic field  $B$  can be obtained by including the Peierls hopping term  $V_\perp = t \exp i\alpha$ ,  $\alpha = (e/\hbar)Ba^2$  into the Hamiltonian (6).

### IV. THE MATRIX $K$

The matrix  $K_{ab}$  is defined in terms of higher moments of the matrices  $v$ :

$$K_{ab} \equiv \langle k_{ab} \rangle \quad (11)$$

Here,  $\langle \dots \rangle$  represents an ensemble average.

For the orthogonal system, the matrix  $k_{ab}^O$  is defined as<sup>17</sup>

$$k_{ab}^O = \sum_{\alpha=1}^L |v_{\alpha a}|^2 |v_{\alpha b}|^2. \quad (12)$$

In the diffusive regime,<sup>4</sup>

$$K_{ab}^O = \frac{1 + \delta_{ab}}{L + 1}. \quad (13)$$

For the unitary models,

$$k_{ab}^U = \sum_{\alpha=1}^L |v_{\alpha a}|^2 |v'_{\alpha b}|^2 \quad (14)$$

and

$$K_{ab}^U = \frac{1}{L}. \quad (15)$$

For the systems with symplectic symmetry the matrix  $k_{ab}^S$  is given<sup>29,30</sup>

$$k_{ab}^S = \sum_{\alpha=1}^L v_{\alpha a}^\dagger v_{\alpha b}^* \bar{v}_{\alpha b} v_{\alpha a}. \quad (16)$$

In this equation, the  $2 \times 2$  matrices  $v^\dagger$ ,  $v^*$  and  $\bar{v}$  are defined in terms of the matrix  $v$ :

$$v = \begin{pmatrix} v_{11} & v_{12} \\ v_{21} & v_{22} \end{pmatrix} \quad v^\dagger = \begin{pmatrix} v_{11}^* & v_{21}^* \\ v_{12}^* & v_{22}^* \end{pmatrix}, \quad (17)$$

and

$$v^* = \begin{pmatrix} v_{11}^* & v_{12}^* \\ v_{21}^* & v_{22}^* \end{pmatrix}, \quad \bar{v} = \begin{pmatrix} v_{22} & -v_{12} \\ -v_{21} & v_{11} \end{pmatrix}. \quad (18)$$

In the diffusive regime,  $K_{ab}^S$  is degenerated diagonal matrix<sup>29</sup> with diagonal elements

$$K_{ab}^S = \frac{2 - \delta_{ab}}{2L - 1}. \quad (19)$$

Our numerical results discussed in Sect. V confirm that the same holds for any disorder strength.

From Eqs. (13,15,19) it follows that

$$\sum_b K_{ab}^O = \sum_b K_{ab}^U = \sum_b K_{ab}^S = 1. \quad (20)$$

We use these relations to test the numerical accuracy of our results.

## V. RESULTS

We consider square samples of the size  $L \times L$  attached to two semi-infinite ideal leads. The size  $L$  increases from  $L = 10$  to  $L = 256$  (S model) up to  $L = 600$  (O model). For each value of  $L$  and  $W$ , we analyze the statistical ensemble of typically  $N_{\text{stat}} \sim 10^4$  samples ( $N_{\text{stat}} \sim 1000 - 4000$  for the largest system size). In numerical calculation, the sample and leads are represented by the  $2N \times 2N$  transfer matrix  $M$  and  $M_0$ , respectively.<sup>31</sup> Following<sup>32</sup>, the conductance is given as a trace of matrices  $L^+MR^+$  and  $L^-MR^-$ , where  $R^{+-}$  ( $L^{+-}$ ) are  $N \times 2N$  ( $2N \times N$ ) matrices composed of right and left eigenvalues of  $M_0$ , respectively. The upper index  $+$  ( $-$ ) indicate the direction of the propagation through the sample. Comparing with Eq. (1) we find

$$L^+MR^+ = v(1 + \lambda)^{-1}v^\dagger \quad (21)$$

and

$$L^-MR^- = v'^\dagger(1 + \lambda)^{-1}v'. \quad (22)$$

Thus, eigenvalues  $\lambda_a$  can be obtained numerically by diagonalizing of the matrices  $L^+MR^+$  and  $L^-MR^-$ . Matrices  $v$  and  $v'$  consist of corresponding eigenvectors. Details of numerical method are given in Ref.<sup>20</sup> Mean values,  $K_{11}$  and  $K_{12}$  were calculated as an average over the statistical ensemble

$$K_{ab} = \frac{1}{N_{\text{stat}}} \sum_{i=1}^{N_{\text{stat}}} k_{ab}^{(i)}. \quad (23)$$

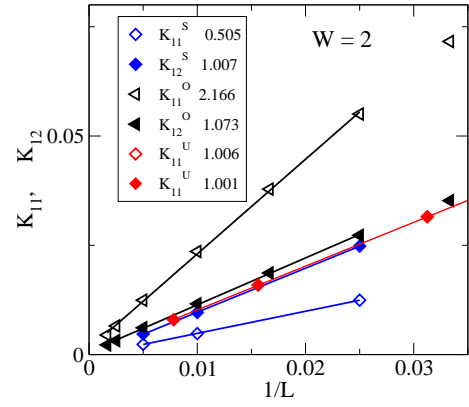


FIG. 1: (Color online)  $K_{11}$  and  $K_{12}$  as a function of the system size for square lattice  $L \times L$  for the symplectic (S) and orthogonal (O) s and unitary (U) systems. The disorder  $W = 2$ . Solid lines are linear fits with slopes given in the legend.

Obtained data for  $k_{ab}$  were also used for the calculation of probability distributions.

As noted in Section IV,  $K_{ab}^S$  are  $2 \times 2$  matrices. Numerical data confirm that, with the relative accuracy of  $10^{-3}$ , these matrices remain diagonal degenerate for each value of the disorder and all size of the system.

### A. Diffusive regime

We first verify the prediction of the DMPK equation for the diffusive regime. In Fig. 1 we show the  $L$  dependence of parameters  $K_{11}$  and  $K_{12}$  for the orthogonal and symplectic system with disorder  $W = 2$ . The system is in the diffusive regime (the conductance  $g$  varies between 4.9 and 5.03 for the orthogonal model, and increases from 7 to 11 for the S model). Linear fits shown by solid lines confirm that both  $K_{11}$  and  $K_{12} \sim 1/L$  and  $\gamma$  equals to the symmetry parameter  $\beta$  in the diffusive regime. The spatial distribution of electrons is homogeneous and no additional parameter must be introduced into the model. The transport is universal, the only model parameter in the DMPK is the ratio  $L_z/\ell$  of the system length to the mean free path. Although the DMPK was derived only for the quasi-one dimensional systems, our data show that relations (13,15,19) are valid also for the square samples.

### B. Insulating regime

In the limit of strong disorder, we expect that  $K_{aa}$  depend on the index  $a$  and  $K_{aa} \sim O(1)$ . Contrary, off-diagonal elements  $K_{ab}$ ,  $a \neq b$ , should decrease to zero,  $K_{ab} \sim 1/L$  ( $a \neq b$ ) so that  $\gamma \sim 1/L$  decreases to zero when the size of the system increases.<sup>17</sup>

Figure 2 shows the  $L$  dependence of  $K_{11}^O$  and  $K_{12}^O$  for orthogonal systems with various strength of the disorder.

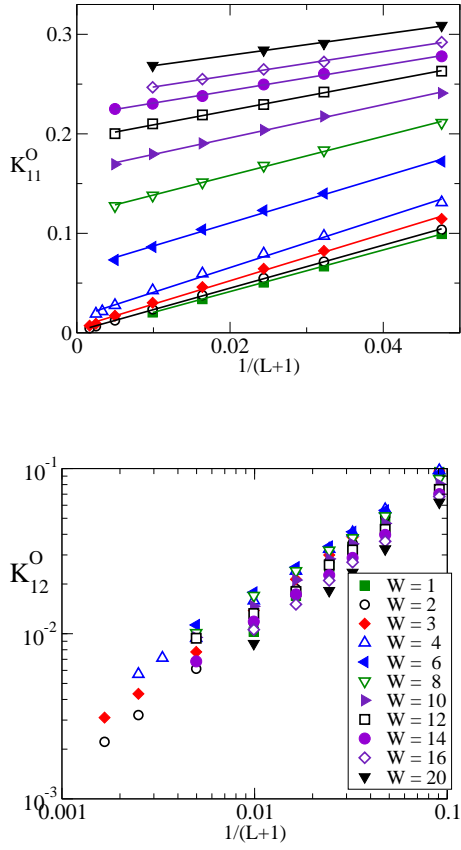


FIG. 2: (Color online) The size dependence of  $K_{11}$  (top) and  $K_{12}$  (bottom) for the 2D orthogonal model for various strength of the disorder (given in the legend of bottom panel).  $K_{11}$  converges to the non-zero limit when  $L \rightarrow \infty$  for each disorder strength. This limiting value, however, is too small to be observable numerically for weak disorder within the considered size of the system.  $K_{12}$  decreases to zero for any value of the disorder  $W$ .

Similarly to the 3D orthogonal model discussed in<sup>20</sup>, both  $K_{11}^O$  and  $K_{12}^O$  are linear functions of  $1/(L+1)$ . Since no metallic regime exists for the non-zero disorder, we expect that  $K_{11}^O$  converges to the nonzero value in the limit of  $L \rightarrow \infty$  for all values of  $W$ ,

$$K_{11}^O = K_{11}^{O\infty} + \frac{c}{L+1}. \quad (24)$$

The limiting value  $K_{11}^{O\infty}$  can be easily calculated numerically for strong disorder. This is more difficult for weak disorder ( $W < 4$ ), since  $K_{11}^{O\infty}$  becomes smaller than the inverse of the accessible sample size.

Similar data (not shown) were obtained also for the symplectic models.

### C. Critical regime (symplectic models)

Critical regime exists only for the S systems. In the critical regime,  $W = W_c$  we found that both  $K_{11}^S$  and

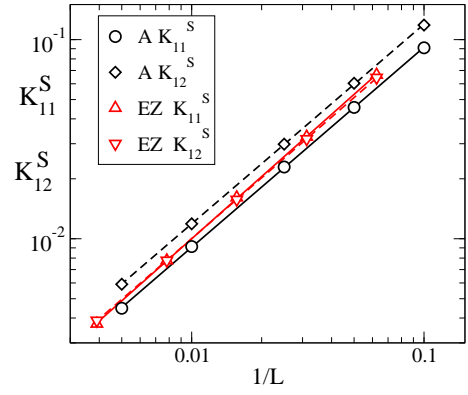


FIG. 3: (Color online) The size dependence  $K_{11}$  and  $K_{12}$  at the critical point for the symplectic (Ando and EZ model) models. Solid and dashed lines are power fits  $K_{1a}^S \propto L^{-\alpha}$  ( $a = 1, 2$ ) with the exponent  $\alpha \approx 1.003 - 1.005$ .

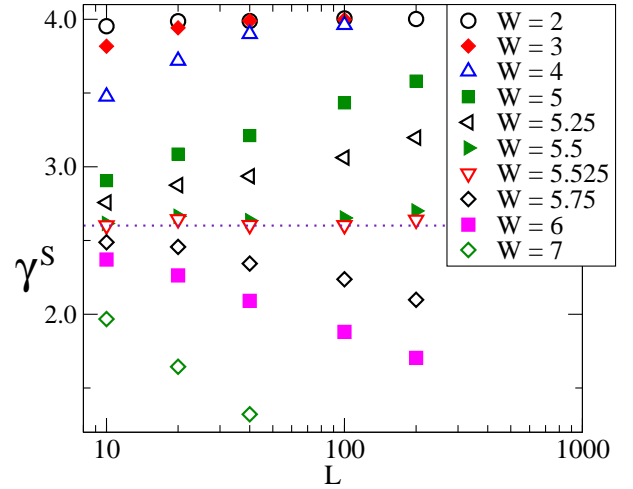


FIG. 4: (Color online) The size dependence of the parameter  $\gamma^S = 2K_{12}^S/K_{11}^S$  for the Ando model. In the metallic regime, ( $W < W_c = 5.525$ ),  $\gamma^S$  slowly increases when  $L$  increases and converges to its isotropic value  $\gamma^S = 4$ . In the localized regime ( $W > W_c = 5.525$ ),  $\gamma^S$  decreases to zero when the size of the system increases. At the critical point,  $\gamma^S$  does not depend on  $L$ . The  $L$ -independent critical value of  $\gamma^S \approx 2.60$  (dotted line) is plotted by dot line.

$K_{12}^S$  decreases at the critical point to zero

$$K_{11}^S(W = W_c), \quad K_{12}^S(W = W_c) \propto \frac{1}{L} \quad (25)$$

(Fig. 3), so that  $\gamma^S$  reaches a critical value,  $\gamma_c^S = 2K_{12}^S/K_{11}^S$  which does not depend on the size of the system

$$\gamma_c^S = \text{const.} \quad (26)$$

As shown in Fig. 3, the critical value  $\gamma_c^S$  is not universal but depend on the model. We obtain  $\gamma_c^S = 2.601$  for the

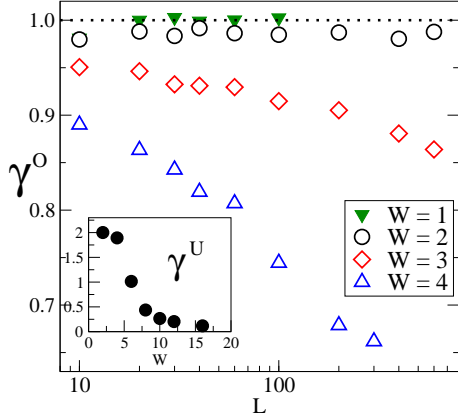


FIG. 5: (Color online) The size dependence of the parameter  $\gamma^O = 2K_{12}^O/K_{11}^O$  for the 2D orthogonal model. We expect that  $\gamma^O$  decreases to zero for any value of the disorder  $W$ . However, the size of the system  $L$  is not sufficient to see this decrease when the disorder is small. Instead, we observe the diffusive limit  $\gamma^O \approx 1$ . Only for sufficiently strong disorder,  $\gamma^O$  decreases to zero. In contrast to the symplectic model (Fig. 4) there is no indication for the existence of the critical point where  $\gamma^O$  converge to the  $L$ -independent limit. Inset shows the disorder dependence of  $\gamma^U$  for the unitary ensembles ( $L = 128$ ,  $\alpha = 1/8$ ).

Ando model, and 1.795 for the Evangelou-Ziman model.

Figure 4 shows that the length and disorder dependence of parameter  $\gamma^S$  can be, at least in principle, used for the estimation of critical parameters in the same way as mean conductance of the smallest Lyapunov exponent. For very weak disorder, we find that  $\gamma^S$  only weakly depends on the size of the system and increases to the metallic limit  $\gamma = 4$  when  $L$  increases to infinity, indicating that the system is in the metallic regime. For stronger disorder,  $\gamma^S \propto 1/L$  decreases to zero when the size of the system increases, in agreement with the prediction of the theory.<sup>17</sup> We found the critical regime between these two limits, where  $\gamma^S$  converges to the size-independent constant  $\gamma_c^S \approx 2.60$  (obtained already in Fig. 3) when  $W = W_c$ .

For comparison, we show in Fig. 5 data for  $\gamma^O$  calculated for the 2D orthogonal model. We found no critical regime. Although  $\gamma^O \approx 1$  for weak disorder, we expect that this is the finite size effect, and  $\gamma^O$  will decrease to zero for each disorder strength when  $L$  increases.<sup>8</sup>

#### D. The universality

With two new parameters  $K_{11}$  and  $\gamma$ , we must verify if the transport properties of the system are still maintained by only a single parameter.<sup>8</sup> In the metallic regime, the answer is trivial since the entire matrix  $K$  reduces to model-independent numbers given by Eqs.

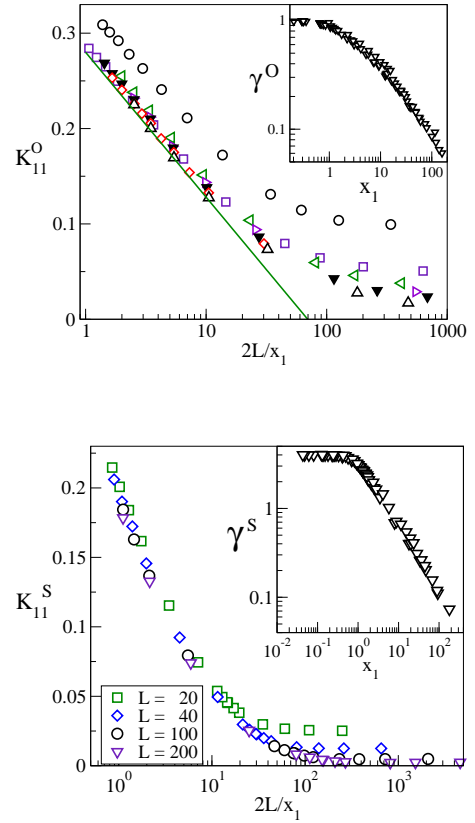


FIG. 6: (Color online)  $K_{11}$  as a function of the localization length  $\xi$  (estimated as  $\xi = 2L/x_1$ ) for the 2D orthogonal model (top) and the 2D symplectic model (bottom). The strength of the disorder varies between  $W = 1$  and  $W = 16$  in both Figures. For strong disorder ( $2L/x_1 \rightarrow 0$ ) data converge to the universal curve (solid line is a function  $0.288 - 0.066 \ln \xi$  for the orthogonal model). Insets in both panels show that  $\gamma$  is an unambiguous function of  $x_1$ .

(13,15,19). The universality of the critical regime was shown in the previous section. Here, we concentrate on the localized regime, where we expect that  $K_{11}$  becomes an unambiguous function of the localization length.<sup>20</sup> The last can be estimated from the smallest parameter  $x_1$ ,

$$\xi = \frac{2L}{x_1}. \quad (27)$$

In Fig. 6 we plot  $K_{11}$  as a function of  $\xi$  for the orthogonal and symplectic Ando models. Data confirm that the parameter  $K_{11}$  becomes an linear function of  $\ln \xi$  with increasing system size and converge to the system-size independent limit when  $L \rightarrow \infty$ .

Two inset of Fig. 6, show that the parameter  $\gamma$  is an unambiguous function of  $x_1$  in all three regimes. In the localized regime, when  $x_1 \sim L$ , data confirm that  $\gamma \sim 1/L$ , consistent with prediction of the Muttalib's theory.

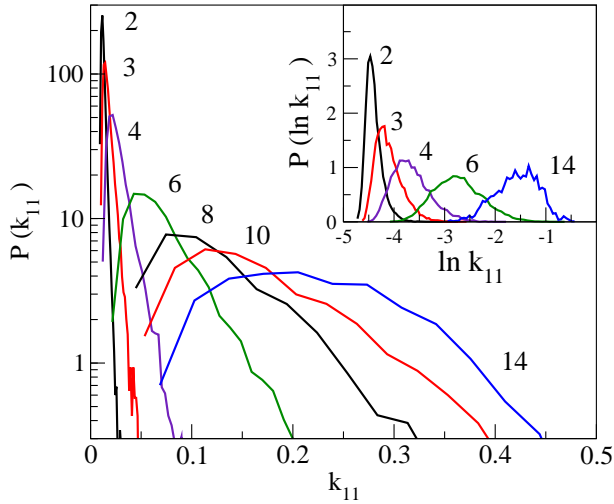


FIG. 7: (Color online) The probability distribution of  $k_{11}$  for the 2D orthogonal model with various disorder strength (given in the figure). The size of the system  $L = 200$ . Inset shows the distributions  $P(\ln K_{11})$ . Data confirm that  $k_{11}$  is a good statistical variable with a well defined mean value and variance.

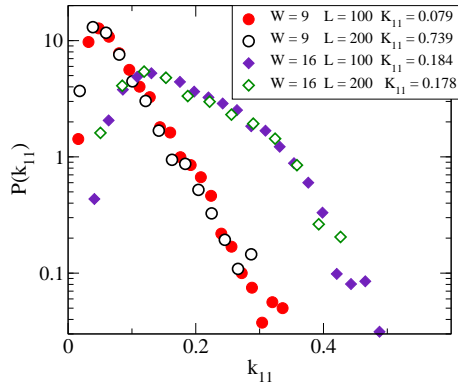


FIG. 8: (Color online) The probability distribution of  $k_{11}$  in the strongly localized regime for the Ando model. The mean value  $K_{11}$  is given in the legend.

### E. Statistical properties of $k_{11}$

In the previous analysis we dealt only with mean values of  $K_{11}$  and  $K_{12}$ . Since both  $k_{11}$  and  $k_{12}$  are statistical variables, we must also to study their statistical properties. Figure 7 shows the probability distribution of parameter  $k_{11}$  and  $\ln k_{11}$  for the 2D orthogonal model. For each disorder, the mean value can be identified with the most probable value. In the localized limit, both  $K_{11}$  and  $\text{var } k_{11}$  are of order of unity, and the distribution  $P(k_{11})$  becomes size independent (Fig. 8).

In Fig. 9 we plot the probability distribution of  $k_{11}$  for the symplectic Ando model in the critical and metallic

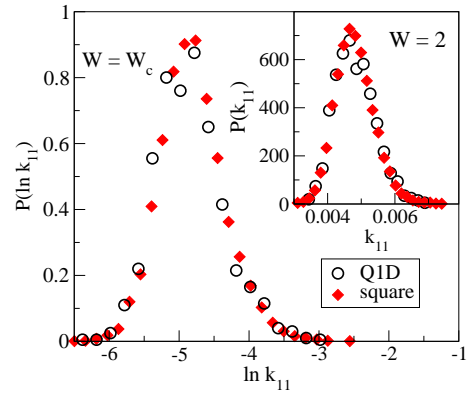


FIG. 9: (Color online) The probability distribution of  $k_{11}$  for the 2D Ando model at the critical point  $W = W_c = 5.525$  and in the metallic regime ( $W = 2$ , inset). Both the square samples  $100 \times 100$  and Q1D samples  $100 \times 5000$  are considered.

regime. We demonstrate that the distributions for the square sample  $L \times L$  with quasi-one dimensional systems are almost identical.

### F. Correlation $g$ vs $k_{11}$

We have shown that  $K_{11} \rightarrow 0$  in the metallic regime but  $K_{11} \sim O(1)$  in the insulator. Small values of  $K_{11}$  indicate that the mean conductance of the system is large. Contrary, large values of  $K_{11}$  correspond to systems with small mean conductance. This is in agreement with our expectation: small conductance means that the electron has problems to go through the sample. When it finally reaches the opposite side, its spatial distribution is not homogeneous any more.

However, the correspondence large  $k_{11}$  - small  $g$  holds only for mean values of these parameters. As shown in Fig. 10, the values of  $g$  and  $k_{11}$  for a given sample are not correlated within a given statistical ensemble: small values  $g \ll \langle g \rangle$  can be accompanied with any value of  $k_{11}$  - either small  $k_{11} \ll K_{11}$  or large  $k_{11} \gg K_{11}$ . The absence of the correlation observed in both the metallic and in strongly localized regime, confirms that the statistical fluctuations of  $k_{11}$  do not affect the mean value of the conductance.

## VI. CONCLUSION

The electron transport through disordered system is determined by spatial distribution of the electron inside the disordered sample, which can be measured by parameters  $K_{11}$  and  $\gamma$ . Our aim in this paper was to investigate how these two parameters depend on the size of the system, strength of the disorder and physical symmetry of the model. We concentrated on 2D disordered systems. In order to better understand the role of the disorder, we

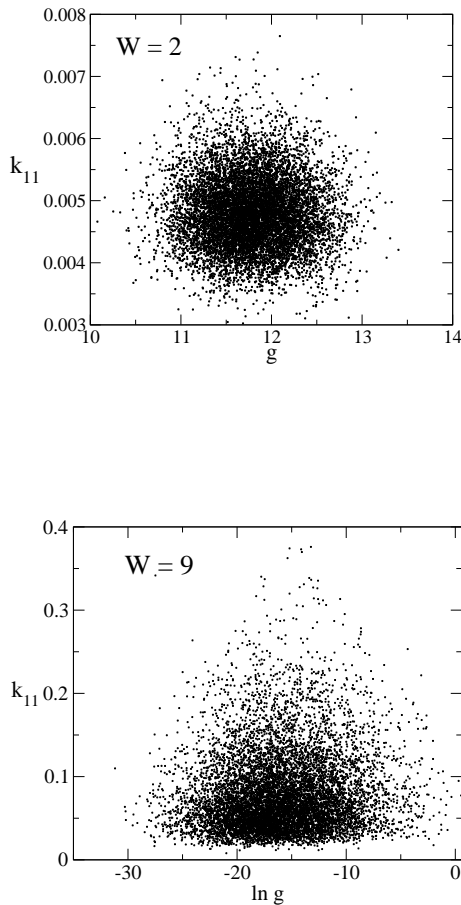


FIG. 10: 2D Ando model:  $k_{11}$  as a function of the conductance statistical ensemble of  $N_{\text{stat}} = 10^4$  samples with disorder  $W = 2$  (top) and  $W = 9$  (bottom). The size of the system  $L = 100$ .

compare numerical data for the orthogonal and symplectic physical symmetry. For completeness, we add also a few data for the unitary ensemble.

In the diffusive regime, the size dependence of both parameters follow the analytical relations given by the theory of DMPK equation. In particular,  $\gamma$  equals to the symmetry parameter  $\beta$ . In the localized regime,  $K_{11}$  converges to the size independent limit and  $\gamma \sim 1/L$ .

For the symplectic models, which exhibit the metal-insulator transition, we analyze the size dependence of both parameters and we found that  $\gamma$  possesses a critical value  $\gamma_c$  when disorder  $W = W_c$ . Also, we found no significant difference between the values of  $K$  for the two dimensional and quasi-one dimensional systems. No critical value was found for the orthogonal model.

We also found that  $K_{11}$  is an unambiguous function of the localization length  $\xi$  and  $\gamma$  is uniquely given by the parameter  $x_1$ . Therefore, the use of these parameters does not contradict the single parameter scaling theory.

Since the elements of matrices  $k$  are given by elements of statistical matrices  $v$ , they are also statistical variables. Fortunately, analysis of their probability distributions confirm that their mean values are good representatives of the statistical ensembles. We found no statistical correlations between the conductance and  $k_{11}$ . Therefore, we conclude that mean values,  $K_{11}$  and  $K_{12}$ , and, consequently,  $\gamma = 2K_{12}/K_{11}$ , are physical parameters for the description of disordered systems.

**Acknowledgments:** This work was supported by project VEGA 0633/09.

- 
- <sup>1</sup> P. A. Lee and T. V. Ramakrishnan, *Rev. Mod. Phys.* **57**, 287 (1985).  
<sup>2</sup> B. Kramer and A. MacKinnon, *Rep. Prog. Phys.* **56**, 1469 (1993).  
<sup>3</sup> P. W. Anderson, *Phys. Rev.* **109**, 1492 (1958).  
<sup>4</sup> O. N. Dorokhov, *JETP Lett.* **36**, 318 (1982); P. A. Mello, P. Pereyra and N. Kumar, *Ann. Phys. (N.Y.)* **181**, 290 (1988).  
<sup>5</sup> B.L. Altshuler, *JETP Lett.* **41**, 648 (1985); P.A. Lee and A.D. Stone, *Phys. Rev. Lett.* **55**, 1622 (1985).  
<sup>6</sup> J.-L. Pichard, in B. Kramer (ed.) *Quantum Coherence in Mesoscopic Systems* NATO ASI **254**, Plenum Press NY and London (1991).  
<sup>7</sup> C. W. J. Beenakker, *Rev. Mod. Phys.* **69** (1997) 731; C. W. J. Beenakker and B. Rejaei, *Phys. Rev. Lett.* **71**, 3689 (1993); *Phys. Rev. B* **49**, 7499 (1994).  
<sup>8</sup> E. Abrahams, P. W. Anderson, D. C. Licciardello, T. V. Ramakrishnan, *Phys. Rev. Lett.* **42**, 673 (1979); A. MacKinnon, B. Kramer, *Phys. Rev. Lett.* **47**, 1546 (1981).  
<sup>9</sup> F. Evers and A. Mirlin, *Rev. Mod. Phys.* **80** (2008) 1355.  
<sup>10</sup> A. M. Somoza, M. Ortuno, J. Prior, *Phys. Rev. Lett.* **99** (2007) 116602.  
<sup>11</sup> A. Garcia-Garcia, *Phys. Rev. Lett.* **100** (2008) 076404.  
<sup>12</sup> P. Markoš, *Phys. Rev. B* **65**, 104207 (2002);  
<sup>13</sup> P. Markoš, *acta physica slovacica* **56** (2006) 561, arXiv:0609580  
<sup>14</sup> J. Prior, A. M. Somoza, M. Ortuno, *EPJ B* **70** (2009) 513.  
<sup>15</sup> A. M. Somoza, J. Prior, M. Ortuo, and I. V. Lerner, *Phys. Rev. B* **80** (2009) 212201.  
<sup>16</sup> Zhenhua Qiao, Yanxia Xing, and Jian Wang, *Phys. Rev. B* **81** (2010) 085114.  
<sup>17</sup> K. A. Muttalib and J. R. Klauder, *Phys. Rev. Lett.* **82**, 4272 (1999).  
<sup>18</sup> P. Markoš, *Physica B* **405**, 3029 (2010).  
<sup>19</sup> P. Markoš, K. A. Muttalib, P. Wölfle and J. R. Klauder, *Europhys. Lett.* **68**, 867 (2004)  
<sup>20</sup> K. A. Muttalib, P. Markoš, P. Wölfle, *Phys. Rev. B* **72** (2005) 125317.  
<sup>21</sup> A. Douglas and K.A. Muttalib, *Phys. Rev. B* **80** (2009) 161102.  
<sup>22</sup> J. Brndiar, R. Derian and P. Markoš, *Phys. Rev. B* **76** (2007) 155320.  
<sup>23</sup> S. N. Evangelou and T. Ziman, *J. Phys. C* **20** L 235 (1987).

- <sup>24</sup> T. Ando, Phys. Rev. B **40**, 5325 (1989)
- <sup>25</sup> P. A. Mello and J.-L. Pichard, Phys. Rev. B **40**, 5276 (1989).
- <sup>26</sup> E. N. Economou and C. M. Soukoulis, Phys. Rev. Lett. **46** (1981) 618; *ibid* **47** (1981) 973 .
- <sup>27</sup> In the absence of the disorder, the  $z$ -component of the wave vector

$$\cos k_z a = \frac{1}{2V_{\parallel}} [E - 2V_{\perp} \cos k_x a]$$

is real for all possible values of  $k_x$  provided that the energy  $E$  is close to the band center  $E = 0$ .

- <sup>28</sup> P. Markoš and L. Schweitzer, J. Phys. A: Math Gen. **39** (2006) 3221.
- <sup>29</sup> A. M. S. Macedo and J. T. Chalker, Phys. Rev. B **46** 14985 (1992).
- <sup>30</sup> P. A. Mello, J. Phys. A: Math. Gen. **23**, 4061 (1990).
- <sup>31</sup> For symplectic models, each element of  $M$  and  $M_0$  is the  $2 \times 2$  matrix.
- <sup>32</sup> J. B. Pendry, A. MacKinnon, P. J. Roberts, Proc. R. Soc. London A **437**, 67 (1992).